AJNR

# MR Imaging of the Human Brain at 1.5 T: Regional Variations in Transverse Relaxation Rates in the Cerebral Cortex

Christos S. Georgiades, Ryuta Itoh, Xavier Golay, Peter C. M. van Zijl and Elias R. Melhem

*AJNR Am J Neuroradiol* 2001, 22 (9) 1732-1737
http://www.ajnr.org/content/22/9/1732

*AJNR Am J Neuroradiol* 22:1732–1737, October 2001

# MR Imaging of the Human Brain at 1.5 T: Regional Variations in Transverse Relaxation Rates in the Cerebral Cortex

Christos S. Georgiades, Ryuta Itoh, Xavier Golay, Peter C. M. van Zijl, and Elias R. Melhem

***BACKGROUND AND PURPOSE:*** **Heterogeneity in cortical signal intensity on T2-weighted MR images has been recently documented. Using a whole-brain, multiecho MR imaging technique, we sought to determine the T2 relaxation times of nine predefined regions in the cerebral cortex and one region in the deep gray matter.**

***METHODS:*** **Ten adult volunteers (nine men and one woman; age range, 18–40 y; average age, 30.8 y) underwent whole-brain imaging with an oblique coronal multiecho 3D Carr-Purcell-Meiboom-Gill MR sequence at 1000/25, 50, 75, 100, 125, and 150 (TR/TE). T2 measurements were obtained, with variably sized regions of interest, from the primary auditory cortex, primary visual cortex, caudate nucleus, superior frontal gyrus, inferior temporal gyrus, middle temporal gyrus, superior temporal gyrus, insula cortex, cingulate gyrus, and hippocampus. Repeated-measures analysis of variance was used to assess the existence of differences in T2 measurements among the anatomic locations.**

***RESULTS:*** **On the basis of T2 measurements, the gray matter structures examined could be divided into four statistically different groups. In ascending order of T2 measurements, the first group consisted of the primary auditory cortex and primary visual cortex; the second group, the caudate nucleus, superior frontal gyrus, inferior temporal gyrus, middle temporal gyrus, and superior temporal gyrus; the third group, the insula cortex; and the fourth group, the cingulate gyrus and hippocampus.**

***CONCLUSION:*** **Significant variation in T2 values among the cortical gray matter of the human brain exists.**

Regional variations in cellular morphology, cytoarchitecture, water content and diffusivity, iron concentration, microcirculation, and metabolic activity of the human brain cortex have been documented by using histologic, physiologic, and imaging studies (1–16). More recently, heterogeneity in cortical signal intensity, particularly in the primary auditory cortex and limbic lobe of the human brain on T2-weighted fast spin-echo and fast fluid-attenuated inversion recovery MR images, respectively, have been attributed to these regional variations (17, 18).

Received January 3, 2001; accepted after revision June 5, 2001.

From the Department of Radiology and Radiological Sciences (C.S.G., R.I., P.C.M.v.Z., E.R.M.), The Johns Hopkins Medical Institution, and the F.M. Kirby Functional Research Center for Functional Brain Imaging (R.I., X.G., P.C.M.v.Z., E.R.M.), Kennedy Krieger Institute, Baltimore, MD.

Supported in part by NIH grants NS31490 and NS37664 (P.C.M.v.Z.).

Address reprint requests to: Elias R. Melhem, MD, Department of Radiology, The Johns Hopkins Hospital, 600 North Wolfe Street, Baltimore, MD 21287-2182.



MR imaging can provide intrinsic tissue parameters, such as longitudinal (ie, T1) and transverse (ie, T2) relaxation times of the human brain, that are influenced by these variations (19). In vivo characterization of normal regional cortical variations in T2 relaxation times may provide insight into neurologic and psychiatric disorders that alter cellular morphology, microcirculation, and iron content (7, 20–23).

Using a whole-brain multiecho MR imaging technique, we sought to determine the T2 relaxation times of nine regions in the cerebral cortex and one region in the deep gray matter. The cortical zones were chosen to represent known variability in cytoarchitecture, iron concentration, and water content. Our null hypothesis was that the T2 relaxation times of the cortical zones do not differ.

## Methods

### *MR Imaging*

Brain MR imaging was performed with a 1.5-T MR system (ACS-NT; Philips Medical Systems, Best, the Netherlands) with a maximum gradient capability of 23 mT/m, slew rate of

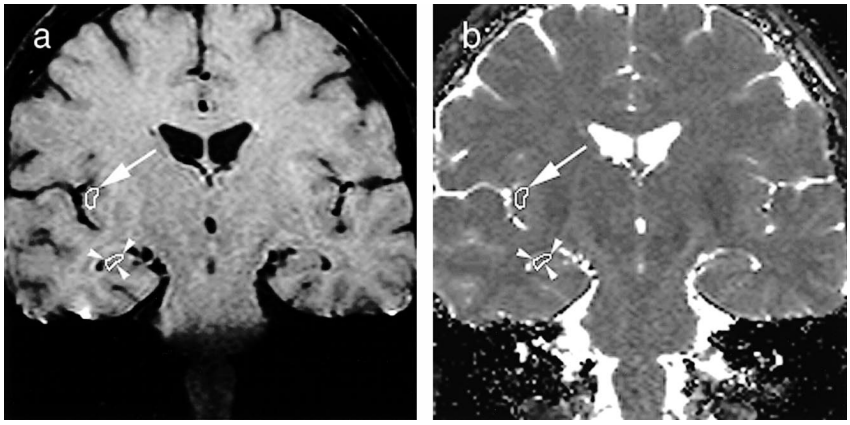


FIG 1. First-echo oblique coronal MR images (1000/25) of the brain, with variably sized ROIs placed in the insular cortex (*arrow*) and hippocampus (*arrowheads*).

*a,* Multiecho 3D CPMG image obtained in a healthy volunteer at the level of the frontal horns of the lateral ventricles.

*b,* Corresponding pixel-by-pixel T2 map.

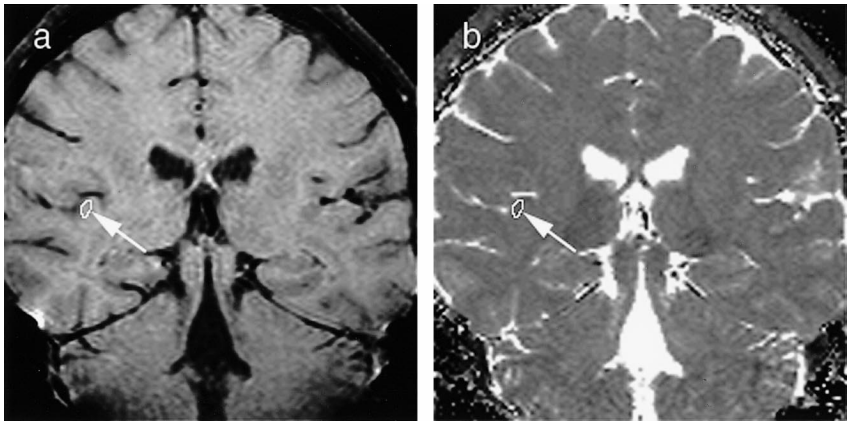


FIG 2. First-echo oblique coronal MR images (1000/25) of the brain, with variably sized ROIs placed in the primary auditory cortex (*arrow*).

*a,* Multiecho 3D CPMG image obtained in a healthy volunteer at the level of the bodies of the lateral ventricles.

*b,* Corresponding pixel-by-pixel T2 map.

103 mT/m/ms, and a quadrature head coil operating in receive mode.

The MR imaging protocol included a sagittal T1-weighted fast field-echo sequence for planning imaging location and an oblique coronal multiecho 3D Carr-Purcell-Meiboom-Gill (CPMG) sequence for generating T2 relaxation maps.

For the sagittal T1-weighted fast field-echo MR imaging, the parameters were as follows: 13/4.6 (TR/TE); number of signals acquired, 1; flip angle, 20°; matrix, 256 × 128; field of view, 250 mm; section thickness, 10 mm; and section gap, 10 mm. According to the reference images, oblique coronal imaging was performed perpendicular to the long axis of the hippocampus (24, 25). Total brain coverage in the oblique coronal plane was achieved in 19 min 51 s by using a multiecho 3D CPMG MR imaging sequence (26). The sequence consisted of 12 spin-echo echo-planar segments (separated by 180 refocusing pulses), with 11 gradient echoes within each segment. The parameters were as follows: 1000/50, 75, 100, 125, and 150; matrix, 256 × 132; 55 3-mm-thick continuous partitions; and rectangular field of view, 256 × 179 mm. The sequence had built-in crusher gradients to suppress signal from free induction decay generated by the multiple 180° refocusing radiofrequency pulses. Specially defined 90°–240°–90° refocusing pulses were used to optimize echo formation while minimizing occurrence of stimulated echoes. From the 3D CPMG MR data, pixel-by-pixel T2 relaxation maps were generated by using a linear (least-squares) fit of the natural logarithmic signal intensity and the proton spin density simultaneously obtained from the intercept with a TE of 0 (27).

### *Subjects*

Ten healthy adult volunteers (nine men and one woman; average age, 30.8 y; age range, 18–40 y) underwent imaging with the aforementioned protocol. The institutional internal review board approved the human-subject protocol, and informed consent was obtained from all participating volunteers.

### *T2 Measurements*

T2 relaxation maps and original 3D CPMG images were transferred to a workstation (Sun ULTRA 2; Sun Microsystems, Mountain View, CA). Two radiologists (C.S.G., R.I.) manually and independently placed variably sized (range, 3.6–29.8 $mm^2$) irregularly shaped regions of interest (ROIs) in the left and right primary auditory cortex, primary visual cortex, caudate nucleus, superior frontal gyrus, inferior temporal gyrus, middle temporal gyrus, superior temporal gyrus, insula cortex, cingulate gyrus, and hippocampus by using commercially available software (EasyVision releases 4.2.1.1; Philips Medical Systems). ROIs were according to predefined anatomic locations agreed on by both observers before the initiation of the study (1, 17). The ROIs were placed on the first echo images from the 3D CPMG sequence because they provided the greatest gray-white matter contrast; the intent was to achieve maximum coverage while avoiding boundaries that could cause partial volume effects from subcortical white matter, CSF, and cortical veins (Figs 1 and 2). The ROIs were then copied onto the corresponding T2 relaxation maps and manually adjusted on the basis of visual inspection, when necessary.

**Test-retest and interrater consistencies in T2 measurements in 10 volunteers**

| Anatomic Location | T2 Relaxation Times (ms) | Coefficient of Reliability | |
|---|---|---|---|
| | | Test-Retest Consistency (%) | Interrater Consistency† (%) |
| Primary auditory cortex | 75.92 (1.48) | 3.0 | 3.0 |
| Primary visual cortex | 77.25 (1.43) | 6.6 | 3.7 |
| Caudate nucleus | 83.38 (1.89) | 2.6 | 2.4 |
| Superior temporal gyrus | 84.38 (2.54) | 6.0 | 5.1 |
| Superior frontal gyrus | 87.72 (1.95) | 3.6 | 3.6 |
| Inferior temporal gyrus | 87.62 (1.90) | 3.8 | 4.1 |
| Middle temporal gyrus | 88.17 (1.97) | 4.7 | 4.0 |
| Insula cortex | 92.62 (3.36) | 5.4 | 2.1 |
| Cingulate gyrus | 101.50 (1.96) | 3.6 | 2.6 |
| Hippocampus | 103.40 (2.54) | 5.7 | 5.0 |

* Numbers in parentheses are the SD.

† For interrater consistency, the interval between first and second measurements was 6 wk.

One of the radiologists (C.S.G.) repeated the T2 measurements from the same T2 relaxation maps after 6 wk to evaluate test-retest consistency.

### *Statistical Analyses*

A repeated-measures analysis of variance was used to assess the existence of differences in the averaged (for two observers) T2 measurements among the different left and right anatomic locations. Paired Bonferroni-Dunn post hoc analysis of the anatomic locations were then performed. *P* values of less than .05 were considered to indicate significant differences. Test-retest and interrater consistencies for the averaged (by left and right side) T2 measurements were evaluated by calculating coefficients of reliability (two times the SD of the mean of the difference between two measurements divided by the mean of both measurements) for each of the anatomic locations.

## Results

MR images obtained with the 3D CPMG sequence and the corresponding calculated T2 relaxation maps showed negligible degrading artifacts related to motion, pulsatility, and susceptibility. The average signal-to-noise ratio from gray matter on the last echo images (TE, 150 ms) was 22.6.

Two hundred T2 measurements were available from 10 anatomic locations, on both the left and right sides of the brain, in 10 volunteers. The measurements had a normal distribution.

On the basis of the results of repeated-measures analysis of variance and paired Bonferroni-Dunn post hoc analyses, the T2 measurements between the left and right sides of the brain for the different anatomic locations did not differ ($P > .1$). This finding was true for both observers.

The highest T2 measurement, averaged for observers and sides, was from the hippocampus (103.40 ms), and the lowest was from the primary auditory cortex (75.92 ms) (Table). On the basis of T2 measurements, the gray matter structures examined could be divided into four statistically different groups. In ascending order of T2 measurements, the first group consisted of the primary auditory cortex and primary visual cortex; the second group, the caudate nucleus, superior frontal gyrus, inferior temporal gyrus, middle temporal gyrus, and superior temporal gyrus; the third group, the insula cortex; and the fourth group, the cingulate gyrus and hippocampus (Fig 3). In the second group, the T2 measurements from the superior frontal gyrus, inferior temporal gyrus, and middle temporal gyrus exceeded those from the superior temporal gyrus and caudate nucleus, but they were not significantly different (Fig 3).

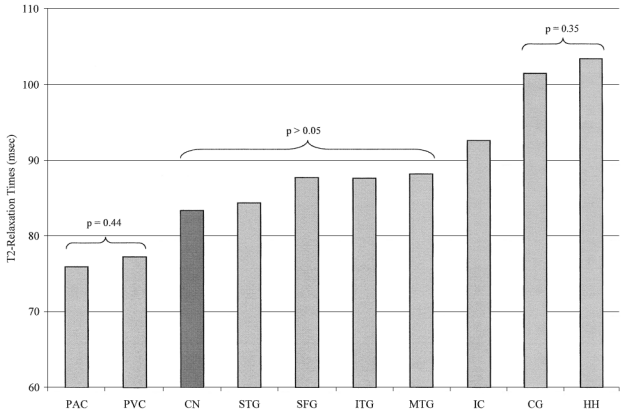


FIG 3. Bar graph of the mean T2 relaxation times in one deep gray matter region, the caudate nucleus (*CN*), and nine cortical regions: primary auditory cortex (*PAC*), primary visual cortex (*PVC*), superior temporal gyrus (*STG*), superior frontal gyrus (*SFG*), inferior temporal gyrus (*ITG*), middle temporal gyrus (*MTG*), insula cortex (*IC*), cingulate gyrus (*CG*), and hippocampus (*HH*). On the basis of the T2 values, the gray matter structures can be divided into four statistically different groups.

Test-retest consistency in the measurement of T2, as assessed by means of the coefficient of reliability, was best for the caudate nucleus (2.6%) and worst for the primary visual cortex (6.6%) (Table). Interrater consistency was best for the insula cortex (2.1%) and worst for superior temporal gyrus (5.1%) (Table).

## Discussion

Although differences in T2 relaxation measures between gray and white matter are well established,

studies of variations in these measures among different areas of cortical gray matter are scarce (3, 28–30). Establishing normative variation in T2 relaxation measures in cortical gray matter may aid in diagnosing and assessing the progression of and the response to therapy for specific neurologic and psychiatric disorders such as Parkinson disease, Alzheimer disease, Huntington disease, and epilepsy (7, 20–23). In addition, mapping of cortical T2 relaxation times may help refine the choice of pulse parameters, especially TE, used in functional MR imaging experiments in different brain regions (15, 16, 31).

Our results confirm previously reported observations of variation in gray matter signal intensity on T2-weighted MR images and provide the intrinsic tissue parameter (T2 relaxation measure) responsible for the variation. Specifically, our findings of corresponding differences in T2 relaxation measures can explain the increases in signal intensity in the hippocampus, cingulate gyrus, and insular cortex on fast fluid-attenuated inversion recovery imaging observed by Hirai et al (18) and decreases in signal intensity in the primary auditory cortex observed by Yoshiura et al (17). Furthermore, Hirai and colleagues' (18) groups of human brain cortical gray matter, based on similarities in contrast-to-noise measurements, are similar to ours. On the basis of findings at visual inspection, Yoshiura et al (17) noted that signal intensity from the primary auditory cortex was lower than that of the middle and superior temporal gyri, and that the signal intensity from the superior temporal gyrus was consistently lower than that of the middle temporal gyrus. They attributed these differences to established variations in the relative development of granular and pyramidal cells among the examined regions (2, 17). Regarding the difference between the middle and superior temporal gyri, our results demonstrate correspondingly higher T2 relaxation measures from the middle temporal gyrus, with a trend toward significance (Table and Fig 3). Our results also are similar to the findings of Whittall et al (3), which indicated that the T2 relaxation measures were significantly higher in the insular cortex and cingulate gyrus compared with those in other cortical gray matter structures, and to the findings of Larsson et al (32), which indicated that in vitro T2 relaxation measures were significantly lower in the primary visual cortex (calcarine cortex) compared with those of other cortical gray matter structures.

Variations in T2 relaxation measures of the gray matter regions evaluated can be attributed to differences in cytoarchitecture, nonheme iron concentration, and water content. Five types of cortices are described on the basis of the relative granular and pyramidal cell development within the cortical layers (2): agranular, frontal, parietal, granular, and polar. That the primary auditory and visual cortices are of the granular type, which is characterized by densely packed granular cells (small neurons), poorly developed third and fourth laminae, and a high degree of myelination, may partly explain their shorter T2 relaxation times (1, 2, 17). A complementary explanation is the well-documented increase in nonheme iron concentrations in the primary auditory and visual cortices (6, 17, 33).

Differences in water content among cortical gray matter structures that are related to variations in cellular composition and extracellular compartment, including vascularization, may partially account for the differences in T2 relaxation measurements. The greater total water content in the insular cortex and cingulate gyrus and the higher density of capillary network in the hippocampus may partly be responsible for the observed increase in T2 relaxation times in those regions (3, 5). Furthermore, the effect of existent variations in the amount of water within myelin bilayers and the differences in the resting oxygen extraction rates on the T2 relaxation measures of cortical gray matter is negligible under normoxic conditions at 1.5 T (3, 28, 34).

The multiexponential T2 decay of free water in a multicompartment environment complicates the in vivo quantification of brain tissue T2 relaxation (35). Thus, the accuracy of this measurement is influenced by the choice of MR pulse sequence and the method for calculating the T2 relaxation measures from the MR imaging data.

MR pulse sequences designed to provide accurate in vivo quantification of T2 relaxation measurements must satisfy the following criteria: 1) elimination of the effects of stimulated echoes on T2 decay; 2) refocusing of the magnetization in the selected section, including dephasing related to time allowed for molecular diffusion through regions of variable magnetic fields; 3) sampling of sufficient number of echoes to adequately characterize the observed decay; and 4) elimination of the effects of magnetization transfer on T2 decay (3, 36).

In this study, we used a whole-brain 3D CPMG MR imaging sequence that was optimized to address the first two criteria. To minimize the contribution of stimulated echoes and to improve complete magnetization refocusing, optimized 90°–240°–90° refocusing pulses were applied by using the quadrature body coil (for better homogeneity). In addition, strong crusher gradients were inserted at either side of every 180° pulse to further diminish stimulated echo effects on absolute T2 quantification. Regarding the third criterion, the 3D CPMG sequence does allow whole-brain imaging and sampling of a sufficient number of echoes (more than four) to adequately characterize the observed T2 decay in less than 20 min (3). The magnetization transfer effect is practically unavoidable in multisection MR imaging and only indirectly influences the absolute T2 relaxation measurement of a given tissue. Furthermore, the effect of T2*, originating from the non-Hahn echoes in each segment of the CPMG, on the T2 relaxation measurements

is undetectable, and the diffusion sensitization (b value) resulting from the readout, phase-encoding, and crusher gradients implemented in this sequence is less than 1 s/mm$^2$ (26). An advantage of the 3D CPMG sequence is that it drastically reduces the effect of inflow on T2 decay commonly encountered in multisection acquisitions; the repeated excitation of a very large volume, and the opposing effects of even (refocusing) and odd (dephasing) echoes of the CPMG sequence, help minimize inflow-related artifacts (37).

The method for calculating T2 relaxation measurements from image data has been validated with phantoms and human volunteers (27). Other factors that can influence the accuracy of the T2 relaxation measurement are related to volume-averaging effects. In this study, use of a relatively small image voxel size (1.0 × 1.3 × 3 mm) and attention to proper ROI placement by both observers helped reduce contamination from adjacent CSF, white matter, and cortical veins.

The study design did not address a few hardware and pulse-design issues that may have a modest influence on our T2 relaxation measurements. These include measurement of noise introduced into the T2 values by slight imperfections in the 180° radio-frequency pulses, correction for T1 relaxation losses resulting from imaging at a finite TR of 1 s, and testing magnetic field ($B_o$) homogeneity and stability just before each experiment (3).

## Conclusion

We demonstrated significant variation in T2 values among the cortical gray matter regions of the human brain at 1.5 T. On the basis of these values, we were able to divide the examined regions into four distinct groups with similar morphologic and physiologic characteristics. We also presented a clinically feasible whole-brain multiecho 3D MR imaging technique that fulfills most of the criteria for accurate in vivo quantification of T2 relaxation.

## References


1. Williams PL, Warwick R. ***Functional Neuroanatomy of Man.*** Philadelphia, Pa: Saunders; 1975
2. von Economo C, Koskinas GH. ***Die Cytoarchitektonic der Hirnrinde des Erwachsenen Menschen.*** Wien-Berlin, Germany: Springer-Verlag; 1925
3. Whittall KP, MacKay AL, Graeb DA, Nugent RA, Li DKB, Paty DW. **In vivo measurement of T2 distributions and water contents in normal human brain.** *Magn Reson Med* 1997;37:34–43
4. Torak RM, Alcala H, Gado M, Buron R. **Correlative assay of computerized cranial tomography (CCT) water content and specific gravity in normal and pathological postmortem brain.** *J Neuropath Exp Neurol* 1976;35:385–392
5. Duvernoy H, Delon S, Vannson JL. **Cortical blood vessels of the human brain.** *Brain Res Bull* 1981;7:519–579
6. Hallgren B, Sourander P. **The effect of age on the non-heme iron in the human brain.** *J Neurochem* 1958;3:41–51
7. Vymazal J, Brooks RA, Patronas N, Hajek M, Bulte JWM, Di Chiro GD. **Magnetic resonance imaging of brain iron in health and disease.** *J Neurol Sci* 1995;134(suppl):19–26
8. Hill JM. **The distribution of iron in the brain.** In: Youdim MBH, ed. *Brain Iron: Neurochemical and Behavioral Aspects.* London, England: Taylor & Francis; 1988;1–24
9. Vymazal J, Hajeck M, Patronas N, et al. **The quantitative relation between T1-weighted and T2-weighted MRI of normal gray matter and iron concentration.** *J Magn Reson Imaging* 1995;5:554–560
10. Bizzi A, Brooks RA, Brunetti A, et al. **Role of iron and ferritin in MR imaging of the brain: a study in primates at different field strengths.** *Radiology* 1990;177:59–65
11. Vymazal J, Brooks RA, Baumgarner C, et al. **The relation between brain iron and NMR relaxation times: an in vitro study.** *Magn Reson Med* 1996;35:56–61
12. Bartzokis G, Beckson M, Hance DB, Marx P, Foster JA, Marder SR. **MR evaluation of age-related increase of brain iron in young adult and older normal males.** *Magn Reson Imaging* 1997;15:29–35
13. Ye FQ, Martin WRW, Allen PS. **Estimation of the iron concentration in excised gray matter by means of proton relaxation measurements.** *Magn Reson Med* 1996;35:285–289
14. Ye FQ, Martin WRW, Allen PS. **Estimation of brain iron in vivo by means of the interecho time dependence of image contrast.** *Magn Reson Med* 1996;36:153–158
15. van Zijl PCM, Eleff SM, Ulatowski JA, et al. **Quantitative assessment of blood flow, blood volume, and blood oxygenation effects in functional magnetic resonance imaging.** *Nature Med* 1998;4:159–167
16. Oja JME, Gillen J, Kauppinen RA, Kraut M, van Zijl PCM. **Determination of oxygen extraction ratios by magnetic resonance imaging.** *J Cereb Blood Flow Metab* 1999;19:1289–1295
17. Yoshiura T, Higano S, Rubio A, et al. **Heschl and superior temporal gyri: low signal intensity of the cortex on T2-weighted MR images of normal brain.** *Radiology* 2000;214:217–221
18. Hirai T, Korogi Y, Yoshizumi K, et al. **Limbic lobe of the human brain: evaluation with turbo fluid-attenuated inversion-recovery MR imaging.** *Radiology* 2000;215:470–475
19. Bottomley PA, Hardy CJ, Argersinger RE, Allen-Moore G. **A review of 1H nuclear magnetic resonance relaxation in pathology: are T1 and T2 diagnostic?** *Med Phys* 1987;14:1–37
20. Chen JC, Hardy PA, Kucharczyk W, et al. **MR of human postmortem brain tissue: correlative study between T2 and assays of iron and ferritin in Parkinson and Huntington disease.** *AJNR Am J Neuroradiol* 1993;14:275–281
21. Jackson GD, Connelly A, Duncan JS, et al. **MRI detection of hippocampal pathology in temporal lobe epilepsy: increased sensitivity using quantitative T2 relaxometry.** *Neurology* 1993; 43:1793–1799
22. Ye FQ, Allen PS, Martin WRW. **Basal ganglia iron content in Parkinson's disease measured with magnetic resonance.** *Mov Disord* 1996;11:243–249
23. Gorell JM, Ordidge RJ, Brown GG, Deniau JC, Buderer NM, Helpern JA. **Increased iron-related MRI contrast in the substantia nigra in Parkinson's disease.** *Neurology* 1995;45: 1138–1143
24. Jack C, Twomey C, Zimmeister A, Sharbrough F, Petersen R, Cascino G. **Anterior temporal lobes and hippocampal formations: normative volumetric measurements from MR images in young adults.** *Radiology* 1989;172:549–554
25. Naidich T, Daniels D, Haughton V, Williams A, Pojunas K, Palacios E. **The hippocampal formation and related structures of limbic lobe: anatomic-MR correlation, I: surface features and coronal sections.** *Radiology* 1987;162:747–754
26. Golay X, Silvennoinen MJ, Zhou J, et al. **Measurement of tissue oxygen extraction ratios from venous blood T2: increased precision and validation of principle.** *Magn Reson Med* 2001;46: 282–291
27. Breger RK, Wehrli FW, Charles HC, et al. **Reproducibility of relaxation and spin-density parameters in phantoms and the human brain measured by MR imaging at 1.5 T.** *Magn Reson Med* 1986;3:649–662
28. Zhou J, Golay X, Kauppinen R, et al. **Shorter T2 at 1.5 T in Gray matter in the occipital lobe of normal adult human brain.** *Magn Reson Med* 2001;46:401–406
29. Breger RK, Rimm AA, Fischer ME, Papke RA, Haughton VM. **T1 and T2 measurements on a 1.5-T commercial MR imager.** *Radiology* 1989;171:273–276
30. Chen JC, Hardy PA, Clauberg M, et al. **T2 values in the human brain: comparison with quantitative assays of iron and ferritin.** *Radiology* 1989;173:521–526

31. Yousem DM, Williams SCR, Howard RO, et al. **Functional MR imaging during odor stimulation: preliminary data.** *Radiology* 1997;204:833–838
32. Larsson EM, Englund E, Gyorffy-Wagner Z, Brun A, Cronqvist S, Persson B. **Regional differences in the proton magnetic resonance relaxation times T1 and T2 within the normal human brain.** *Acta Radiol Diagn* 1986;27:231–234
33. Hoek A, Demmel U, Schicha H, Kasperek K, Feinendegen LE. **Trace element concentration in human brain.** *Brain* 1975;98: 49–64
34. Gelman N, Gorell JM, Barker PB, et al. **MR imaging of the human brain at 3.0 T: preliminary report on transverse relaxation rates and relation to estimated iron content.** *Radiology* 1999;210:759–767
35. Whittal KP, Mackay AL, Graeb DA, et al. **In vivo measurement of T2-distributions and water contents in normal human brain.** *Magn Reson Med* 1997;17:34–43
36. Melhem ER, Whitehead RE, Bert RJ, Caruthers SD. **MR imaging of the hippocampus: measurement of T2 with four dual-echo techniques.** *Radiology* 1998;209:551–555
37. Hinks RS, Constable RT. **Gradient moment nulling in fast spin echo.** *Magn Reson Med* 1994;32:698–706